Next-generation all-solid-state battery

Tuan Vo[a,b †], Claas Hüter[b], Stefanie Braun[a], Manuel Torrilhon[a]

[a]Department of Mathematics, Applied and Computational Mathematics (ACoM), RWTH Aachen University, Schinkelstraße 02, 52062 Aachen, Germany
[b]Institute of Energy and Climate Research (IEK-2), Forschungszentrum Jülich, Wilhelm-Johnen-Straße, 52428 Jülich, Germany

Mathematical modelling for the next-generation All-solid-state batteries: Nucleation (SE|SSE)$^{(*)}$-interface

Rechargeable Lithium-ion battery (LIB) is at the heart of every electric vehicle (EV), portable electronic device, and energy storage system [1]. Nowadays, LIBs enable human life more efficient and help to solve global environment issues thanks to EVs' zero emission. However, conventional LIB (c-LIB) is sensible to temperature and pressure, hence, flammable and explosive. This bottleneck is mainly due to liquid-based electrolyte in c-LIBs.

All-solid-state battery (ASSB) is one of promising candidates to overcome bottlenecks of c-LIBs. Thanks to solid-state electrolyte (SSE), ASSB is highly stable towards temperature and pressure. Nevertheless, metallic Li-dendrite triggered at (SE|SSE)-interface is the main drawback as these dendritic threads extrapolate into grain boundary network of SSE, causing crevice, degradation of ionic conductivity, and the probability of short-circuit.

Next-generation All-solid-state battery (ng-ASSB) with a consideration of nucleation criterion defined by

$$a_{\mathsf{Griffith}} := a^* = \arg\min_{a\in\mathbb{R}} \iiint_\Omega f(a,\boldsymbol{u};\lambda,\mu,\boldsymbol{d}\otimes\boldsymbol{d})\,d\Omega - \iint_\Gamma f(a;\gamma)\,d\Gamma\Big|_{\boldsymbol{u}^{(s)}}$$

where, can help to improve ASSB performance.

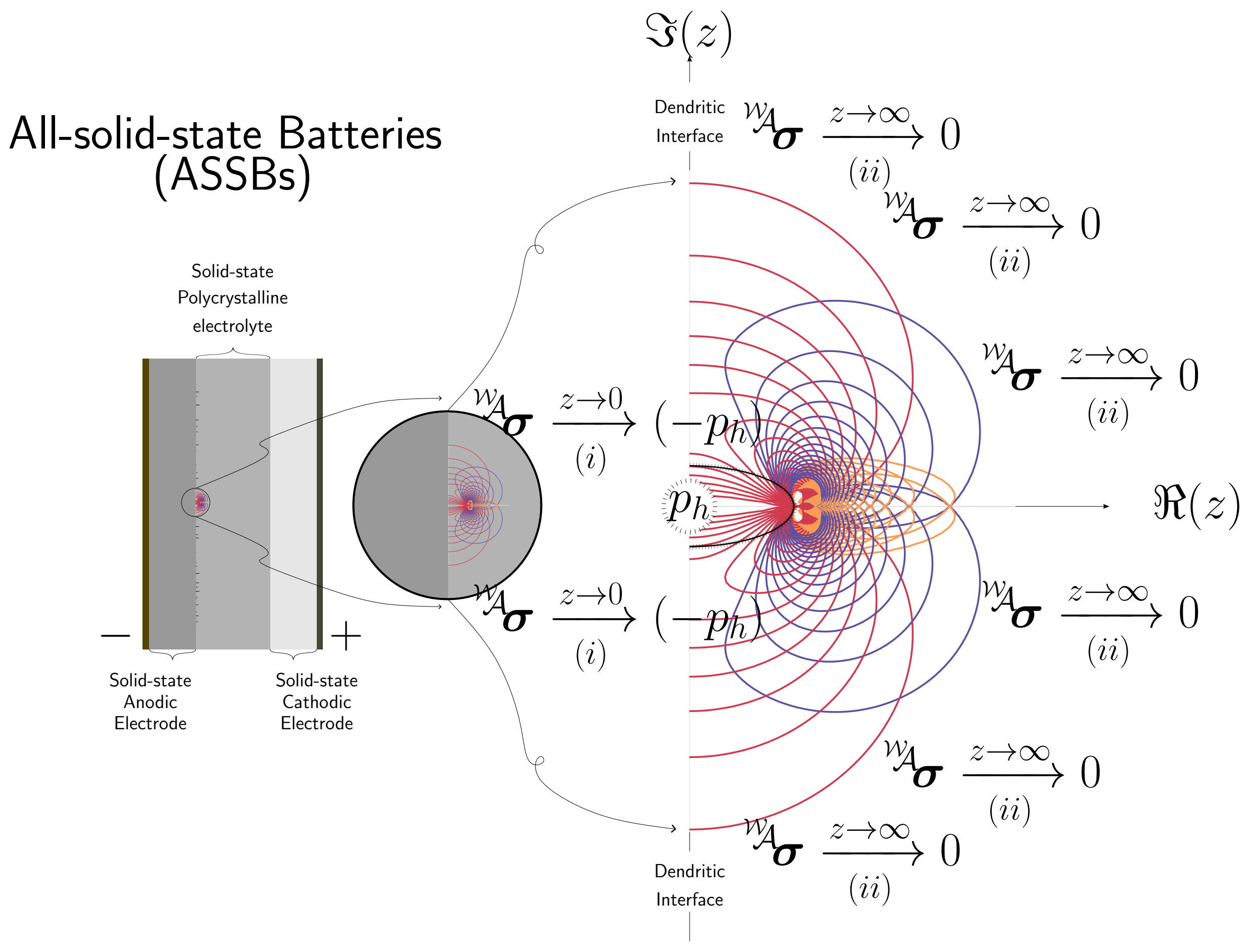

Interface

Interface between solid electrode and solid-state electrolyte (SE|SSE) taking place at space charge layer (SCL) [2] found in ASSBs critically exhibits mechanical and electrochemical instability [3]. This evidence points directly to the fact that the soft metallic li anode is erroneously prone to triggering dendrites, under cycles of electric charge & discharge [4].

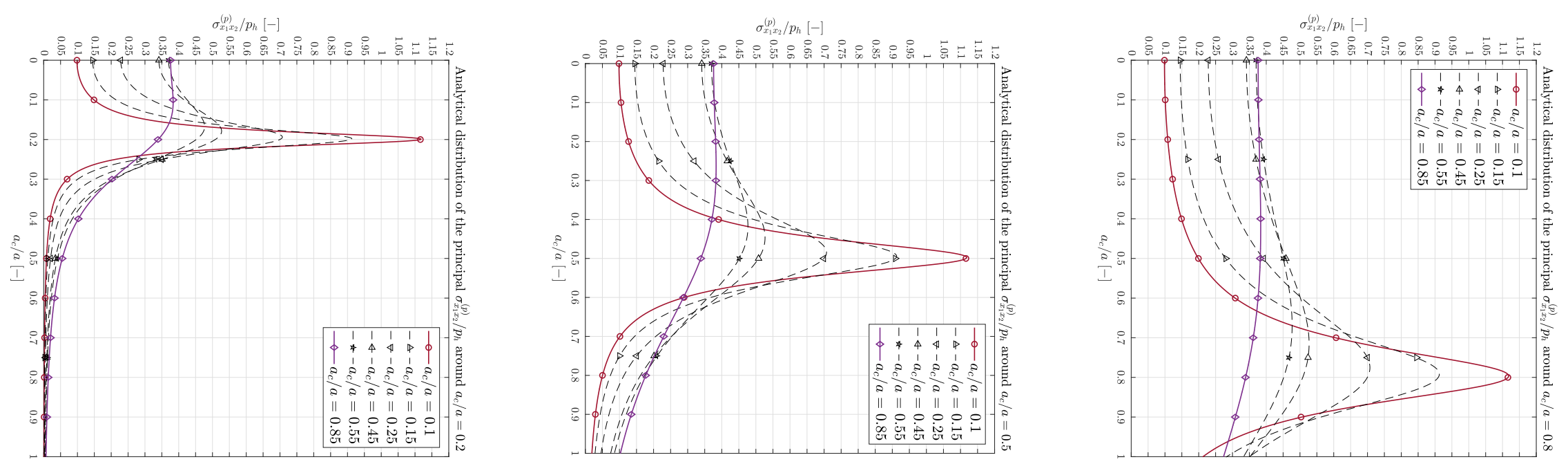

Distribution: ana. max. shear stress ${}^{\mathcal{W}}\!\sigma^{\mathrm{II}}_{x_1x_2}$ around crack tip a_c.

Next-generation All-solid-state battery

Nucleation taking place at critical dendritic (SE|SSE)-interface

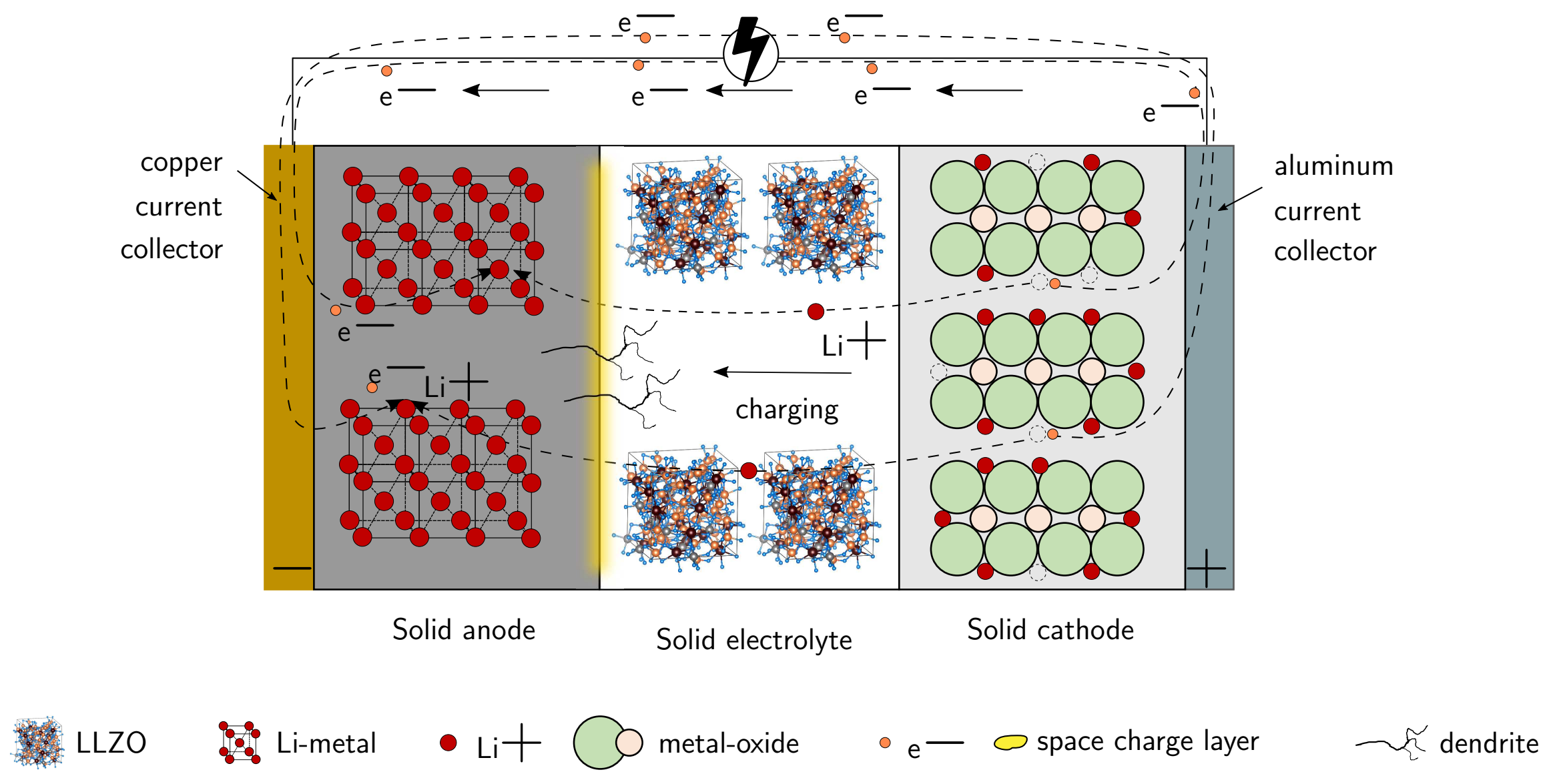

Nucleation taking place at critical dendritic (SE|SSE)-interface
Nucleation taking place at critical dendritic (SE|SSE)-interface

Embedded structural-tensor SSE

Polycrystalline garnet-typed SSE such as LLZO exhibit grain boundaries and various sizes and shapes of grains under microscopic observation. Therefore, this type of microstructure distinctively leads to nuance destruction of ceramic-like materials.

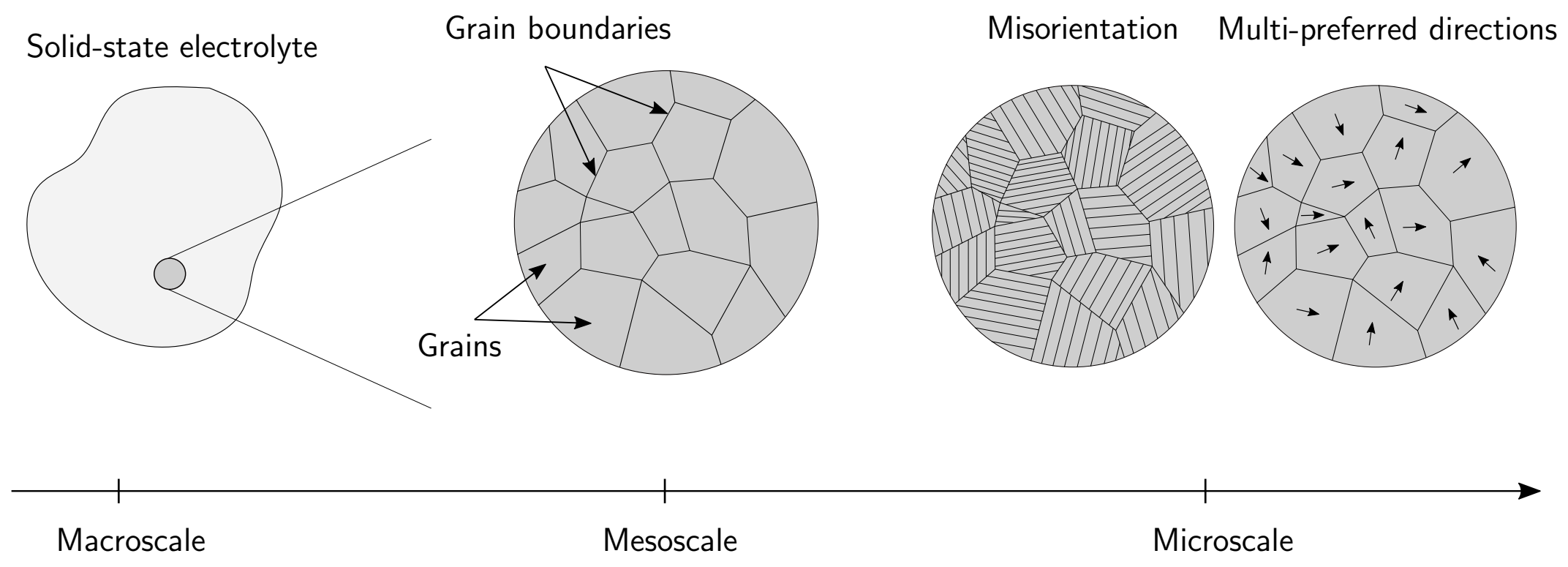

Consequentially, dendrites contribute to degradation of ionic conductivity and trace along grain boundaries in SSE.

Nucleation interface: Taking place at the critical dendritic interface

$$\rho\,\partial^2_{t^2}\boldsymbol{u}^{(s)} + \nabla\cdot\left(\overset{4}{\mathbb{C}}{}^{f^{\mathbb{D}(\Omega)}_{(\lambda,\mu)}} : \nabla\boldsymbol{u}^{(s)}\right) + \rho\nabla V_e = \boldsymbol{0},$$

$$\text{s.t.}\quad a_{\mathsf{Griffith}} := a^* = \arg\min_{a\in\mathbb{R}} \iiint_\Omega f(a,\boldsymbol{u};\lambda,\mu,\boldsymbol{d}\otimes\boldsymbol{d})\,d\Omega - \iint_\Gamma f(a;\gamma)\,d\Gamma\Big|_{\boldsymbol{u}^{(s)}}$$

$$\rho\,\partial^2_{t^2}\boldsymbol{u}^{(s)} + \nabla\cdot\left(\overset{4}{\mathbb{C}}{}^{f^{\mathbb{D}(\Omega)}_{(\lambda,\mu)}} : \nabla\boldsymbol{u}^{(s)}\right) + \rho\nabla V_e = \boldsymbol{0},$$

$$\text{s.t.}\quad a_{\mathsf{Griffith}} := a^* = \arg\min_{a\in\mathbb{R}} \iiint_\Omega f(a,\boldsymbol{u};\lambda,\mu,\boldsymbol{d}\otimes\boldsymbol{d})\,d\Omega - \iint_\Gamma f(a;\gamma)\,d\Gamma\Big|_{\boldsymbol{u}^{(s)}}$$

$$\rho\,\partial^2_{t^2}\boldsymbol{u}^{(s)} + \nabla\cdot\left(\overset{4}{\mathbb{C}}{}^{f^{\mathbb{D}(\Omega)}_{(\lambda,\mu)}} : \nabla\boldsymbol{u}^{(s)}\right) + \rho\nabla V_e = \boldsymbol{0},$$

$$\text{s.t.}\quad a_{\mathsf{Griffith}} := a^* = \arg\min_{a\in\mathbb{R}} \iiint_\Omega f(a,\boldsymbol{u};\lambda,\mu,\boldsymbol{d}\otimes\boldsymbol{d})\,d\Omega - \iint_\Gamma f(a;\gamma)\,d\Gamma\Big|_{\boldsymbol{u}^{(s)}}$$

$$\rho\,\partial^2_{t^2}\boldsymbol{u}^{(s)} + \nabla\cdot\left(\overset{4}{\mathbb{C}}{}^{f^{\mathbb{D}(\Omega)}_{(\lambda,\mu)}} : \nabla\boldsymbol{u}^{(s)}\right) + \rho\nabla V_e = \boldsymbol{0},$$

$$\text{s.t.}\quad a_{\mathsf{Griffith}} := a^* = \arg\min_{a\in\mathbb{R}} \iiint_\Omega f(a,\boldsymbol{u};\lambda,\mu,\boldsymbol{d}\otimes\boldsymbol{d})\,d\Omega - \iint_\Gamma f(a;\gamma)\,d\Gamma\Big|_{\boldsymbol{u}^{(s)}}$$

$$\rho\,\partial^2_{t^2}\boldsymbol{u}^{(s)} + \nabla\cdot\left(\overset{4}{\mathbb{C}}{}^{f^{\mathbb{D}(\Omega)}_{(\lambda,\mu)}} : \nabla\boldsymbol{u}^{(s)}\right) + \rho\nabla V_e = \boldsymbol{0},$$

$$\text{s.t.}\quad a_{\mathsf{Griffith}} := a^* = \arg\min_{a\in\mathbb{R}} \iiint_\Omega f(a,\boldsymbol{u};\lambda,\mu,\boldsymbol{d}\otimes\boldsymbol{d})\,d\Omega - \iint_\Gamma f(a;\gamma)\,d\Gamma\Big|_{\boldsymbol{u}^{(s)}}$$

Therefore

$$\therefore\quad \boxed{a_{\mathsf{Griffith}} := a^* = \arg\min_{a\in\mathbb{R}} \iiint_\Omega f(a,\boldsymbol{u};\lambda,\mu,\boldsymbol{d}\otimes\boldsymbol{d})\,d\Omega - \iint_\Gamma f(a;\gamma)\,d\Gamma\Big|_{\boldsymbol{u}^{(s)}}}$$

Boundary settings

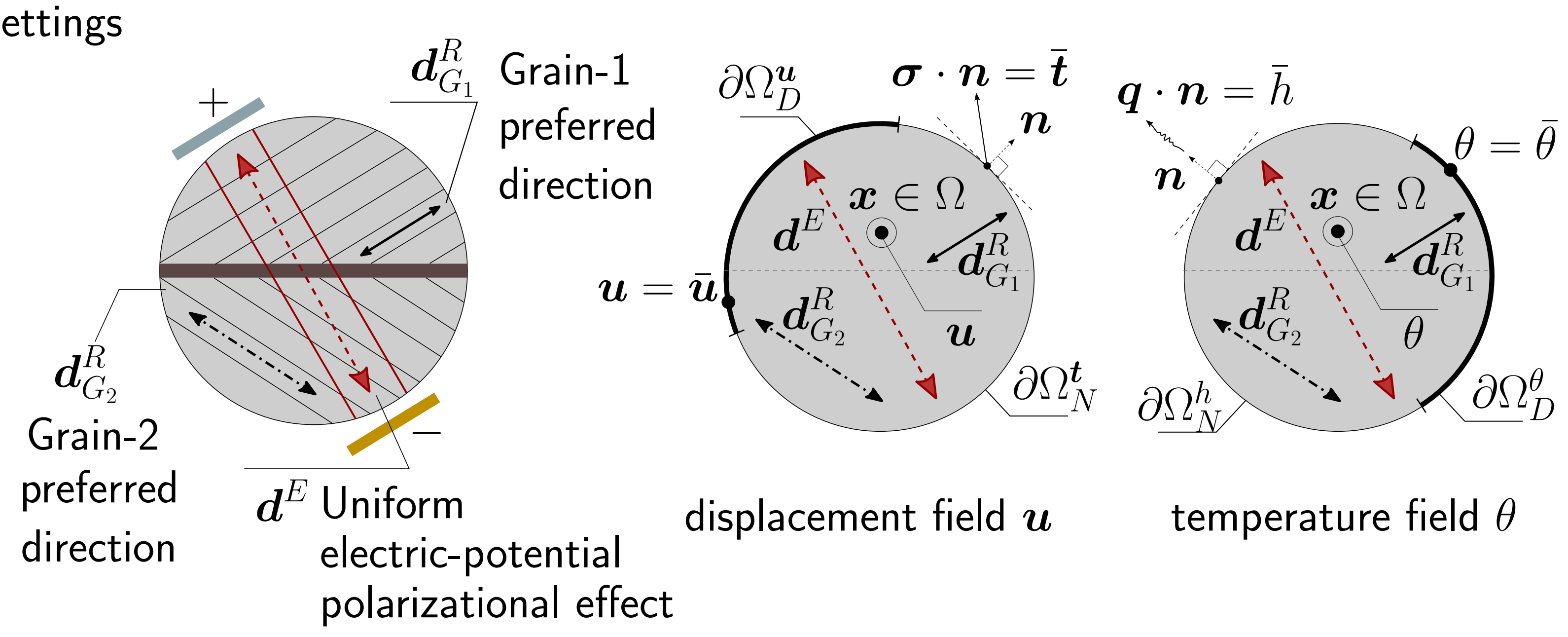

displacement field $\boldsymbol{u}$ temperature field θ

The set of boundary conditions is likewise the path of the pressure-centric dendritic crack.

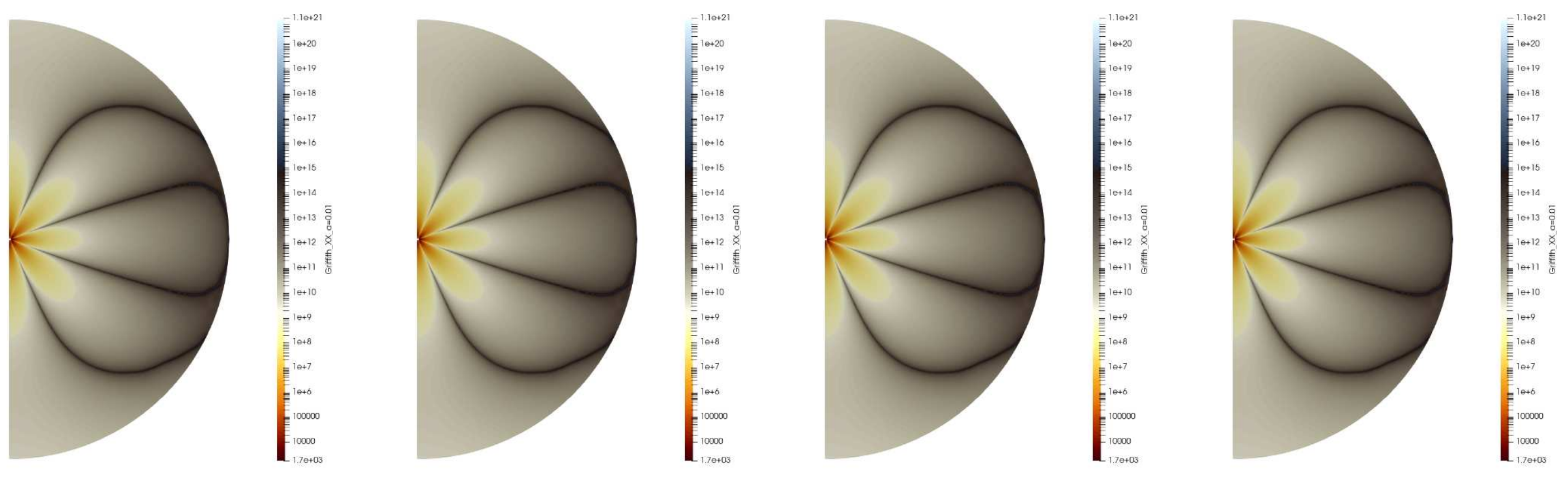

Comparison: Analytical vs. Numerical solutions

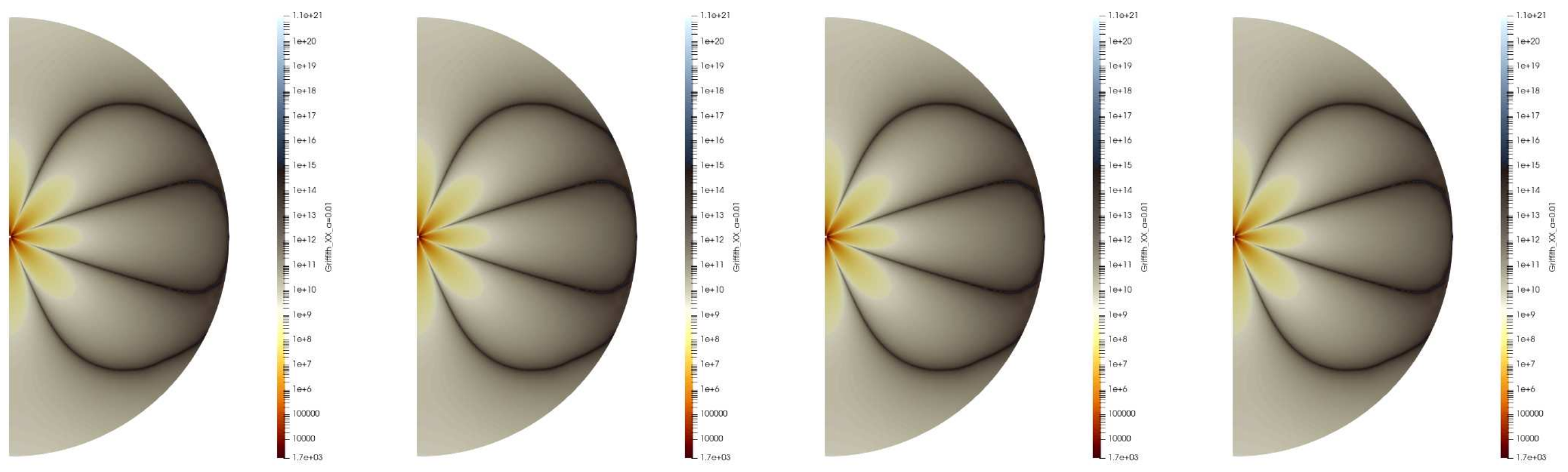

Contact

Tuan Vo
vo@acom.rwth-aachen.de

Scan me

References

[1] **T.Vo**, *Modeling the swelling phenomena of li-ion batt. cells based on a numerical chemo-mech. coupled approach.* MA, Robert Bosch Battery Systems GmbH, 2018.
[2] **S.Braun**, C.Yada and A.Latz, *Thermodynamically consistent model for Space-Charge-Layer formation in a solid electrolyte.* Jr. Phys. Chem., 119, 22281-22288, 2015.
[3] **C.Hüter**, S.Fu, M.Finsterbusch, E.Figgemeier, L.Wells, and R.Spatschek, *Electrode-electrolyte interface stability in solid state electrolyte system: influence of coating thickness under varying residual stresses.* AIMS materials Science, 4(4):867-877, 2017.
[4] **S.Kim**, J.S.Kim, L.Miara, Y.Wang, S.K.Jung, S.Y.Park, Z.Song, H.King, M.Badding, J.M.Chang, V.Roev, G.Yoon, R.Kim, J.H.Kim, K.Yoon, D.Im, and K.Kang, *High-energy and durable li metal batt. using garnet-type solid electrolytes with tailored li-metal compatibility.* Nature Communications, 13(1):1883, 2022.